Mutagenic Specificity of Reductively Activated 1-Nitropyrene in *Escherichia coli*†

Sharon A. Malia and Ashis K. Basu*

Department of Chemistry, University of Connecticut, Storrs, Connecticut 06269

Received August 26, 1994; Revised Manuscript Received October 17, 1994®

ABSTRACT: 1-Nitropyrene (1-NP), the predominant nitropolycyclic hydrocarbon found in diesel exhaust, is a mutagen and tumorigen. Nitroreduction is a major pathway by which 1-NP is metabolized. In order to study the distribution of DNA adducts and the mutational specificity of reductively activated 1-NP, single stranded M13mp18 DNA was treated with *N*-hydroxy-1-aminopyrene generated in situ to give >95% of one major adduct, *N*-(deoxyguanosin-8-yl)-1-aminopyrene. A primer was annealed to DNA containing different levels of adducts, and polymerase extension on these templates was studied. Replication inhibition, primarily at or 3′ to guanine bases, was observed. Transfection of these M13 DNA in *Escherichia coli* indicated a dose-dependent reduction in viability with concomitant enhancement in mutagenesis in the *lacZ* gene fragment. Approximately two adducts per genome constituted one lethal hit (~37% viability). Both survival and mutagenesis were increased when SOS functions of the host cell were induced. *N*-(Deoxyguanosin-8-yl)-1-aminopyrene mutagenesis appeared to be SOS-dependent. With SOS induction, one-base deletions and insertions were the major event (45%), although base substitutions also occurred at high frequency (44%). A major proportion of the point mutations, and particularly one-base deletions and insertions, were detected in 5′-CG, 5′-GC, or 5′-GG sequences. Analysis of the mutation data suggested that *N*-(deoxyguanosin-8-yl)-1-aminopyrene-induced mutations occurred predominantly at the adduct site, but mutations at the base located next to it have been detected at a significant frequency as well. A large fraction of point mutations occurred in a hairpin loop region. If C→T transitions are excluded, most of the point mutations were detected at sites where polymerase arrests occurred. However, neither were the major arrest sites mutational hotspots nor would it be possible to predict mutational sites from the polymerase arrest assay.

Nitrated polycyclic hydrocarbons are formed during combustion processes (Pitts et al., 1978). As a result, these compounds are ubiquitous in the environment and could arise from sources as diverse as grilled food and photocopier toner (Rosenkranz et al., 1980). This group of pollutants has been detected in urban air particulate, coal fly ash, and diesel fuel exhaust (Wang et al., 1980; Rosenkranz, 1982). In addition, their presence in certain cooked foods is a major concern (Ohnishi et al., 1985; El-Bayoumy, 1992). Much attention has been focused on the nitropyrenes since one of the mononitro derivatives, 1-nitropyrene (1-NP),[1] was found in greatest quantities in environmental samples, and the dinitropyrenes are extremely potent mutagens in *Salmonella typhimurium* (Schuetzle, 1983; Rosenkranz & Mermelstein, 1983). Both mononitropyrenes and dinitropyrenes are tumorigenic in animals and have been implicated in the etiology of human breast cancer (Hirose et al., 1984; King, 1988; El-Bayoumy et al., 1988; El-Bayoumy, 1992). In mammalian cells, adducts via ring oxidation have been suspected to contribute toward induction of tumorigenesis by the nitrated pyrenes, but the chemical structures of these adducts have not been determined (El-Bayoumy & Hecht, 1984; Howard et al., 1985; Djurić et al., 1986). Nitroreduction is another major pathway by which these compounds are metabolized (Rosenkranz et al., 1980; Howard & Beland, 1982; Howard et al., 1983a,b). In *Salmonella*, the major DNA adduct formed by 1-NP via nitroreduction is *N*-(deoxyguanosin-8-yl)-1-aminopyrene (dG^{AP}) (Howard et al., 1983b; Heflich et al., 1985). dG^{AP} was detected in mammalian cells as well (Stanton et al., 1985). It is believed that this DNA adduct is formed by the following metabolic route: 1-NP undergoes an enzymatic two-electron reduction to 1-nitrosopyrene (1-NOP) which, in turn, goes through another two-electron reduction to *N*-hydroxy-1-aminopyrene (NHOP). The latter activated species can generate a highly electrophilic nitrenium ion that reacts with guanine (Gua) to form the C8-Gua adduct, Gua^{AP} (Howard et al., 1983b; Heflich et al., 1985, 1986; King, 1988) (Scheme 1).

1-NP has been suggested to be a frame shift mutagen because it reverts *S. typhimurium* strains TA98 and TA1538 more efficiently than TA100 and TA1535 (Rosenkranz & Mermelstein, 1983). The most frequent mutation among the revertants in TA98 is a −2 deletion of GC or CG pair within a CGCGCGCG "hotspot" sequence upstream of the hisD3052 mutation (Bell et al., 1991). Nitroreduction is the metabolic pathway that leads to mutagenesis in *Salmonella* (Howard et al., 1983b). In a forward mutation assay, DNA sequence analysis of 1-NOP-induced mutants in the λ *c*I gene of

† The project described was supported by the National Institute of Environmental Health Sciences (Grant ES05695), National Institutes of Health.

* Address correspondence to this author.

® Abstract published in *Advance ACS Abstracts,* December 1, 1994.

[1] Abbreviations: 1-NP, 1-nitropyrene; 1-NOP, 1-nitrosopyrene; NHOP, *N*-hydroxy-1-aminopyrene; dG^{AP}, *N*-(deoxyguanosin-8-yl)-1-aminopyrene; Gua^{AP}, the corresponding base, *N*-(guanin-8-yl)-1-aminopyrene; AF, 2-aminofluorene; IPTG, isopropyl β-D-thiogalactopyranoside; X-Gal, 5-bromo-4-chloro-3-indolyl β-D-galactopyranoside; ss, single stranded; ds, double stranded; Gua, guanine; Ade, adenine; Cyt, cytosine; Thy, thymine; pfu, plaque forming units; MF, mutation frequency; DTT, dithiothreitol; UV, ultraviolet; BSA, bovine serum albumin; KF (exo⁻), 3′→5′ exonuclease-deficient Klenow fragment; Sequenase version 2.0, a modified 3′→5′ exonuclease-free T7 DNA polymerase.

0006-2960/95/0434-96$09.00/0

Scheme 1: Some of the Known Metabolic Pathways of 1-Nitropyrene

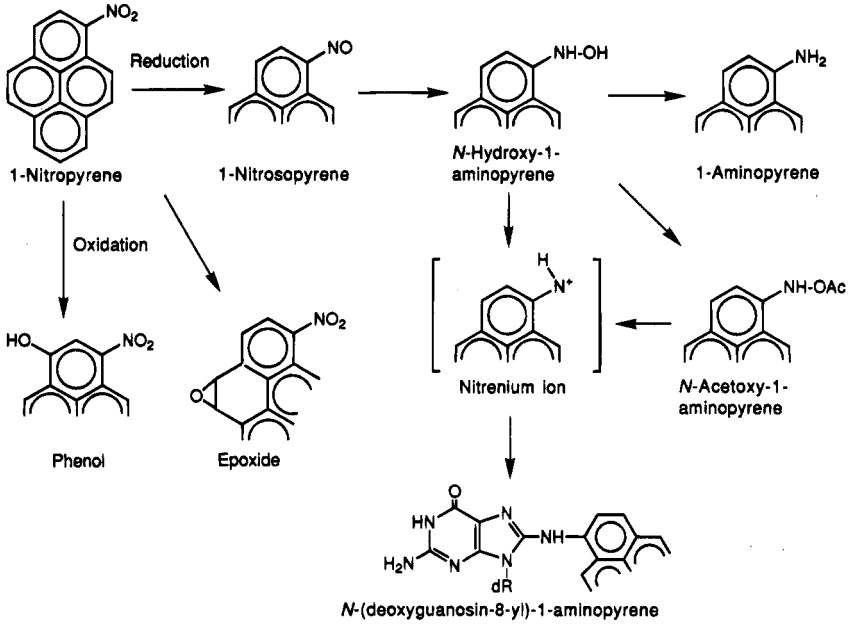

Escherichia coli uvr$^-$ lysogen showed that ~70% mutants were one-base deletions or additions (Stanton et al., 1988). A more recent study in pBR322 gave both −1 deletions and base substitutions, of which G-to-T transversions predominated, but +1 additions were not detected (Melchior et al., 1994). Sequence analyses of NHOP-induced mutants in mammalian cells indicated that base pair substitution, specifically, G·C→T·A transversions, occurred preferentially (Yang et al., 1988; Newton et al., 1992), although in human T-cells G·C→A·T transitions were found most commonly (McGregor et al., 1994). All these investigations were carried out in double stranded (ds) DNA, and no information is available on the consequences of NHOP damage in single stranded (ss) DNA. We believe that it is important to understand the NHOP-induced mutagenesis in both ss and duplex DNA, because most of the DNA in higher organisms remains in its natural ds form whereas long stretches of ss DNA arise due to local unwinding of the duplex during events such as DNA replication and gene expression. Carcinogen−DNA adducts in ss DNA are not amenable to excision repair or homologous recombination as in duplex DNA. Also, an advantage of studying mutagenesis in ss DNA is that each base substitution arises from a defined base rather than a base pair, and therefore there is no ambiguity as to its origin. In addition, the mutational spectra in ss and ds DNA are often significantly different (Gupta et al., 1988).

In the present investigation, we have analyzed the DNA binding spectrum of NHOP, the activated derivative of 1-NP, in ss DNA from bacteriophage M13. We have also evaluated the genotoxicity and mutagenesis of these adducted DNAs upon transfection in *E. coli*. Mutants were scored by using a forward mutation assay that employs partial or complete loss of β-galactosidase activity encoded in the *lacZ* gene fragment of M13mp18 by phenotypic selection of colorless or pale blue plaques. Using this assay, we showed that dG^{AP} mutagenesis is SOS-dependent. dG^{AP} seems to cause a variety of mutations. It would also appear from our data that this adduct can induce both targeted and untargeted mutations. Finally, many point mutations were noted at the sites where polymerase arrests occurred in vitro.

MATERIALS AND METHODS

Materials

E. coli Strains. GW5100 (JM103, P1$^-$) was obtained from G. Walker (MIT, Cambridge, MA). Both DL7 (AB1157, *lacΔU169*, *uvr*$^+$) and DL6 (AB1886, *lacΔU169*, *uvrA*) carrying a chromosomal lac deletion were from J. Essigmann (MIT, Cambridge, MA) [described in Lasko et al. (1988)]. The isogenic strains RW118 (AB1157, *araD139*, *sulA211*) and RW120 (RW118, Δ(*umuDC*)*595::cat*) were from T. Nohmi (National Institute of Hygienic Sciences, Tokyo, Japan).

[4,5,9,10-^{3}H]-1-NOP (specific activity 217 mCi/mmol) was a gift from Dr. Frederick Beland (NCTR, Jefferson, AK). It was >96% pure by HPLC analysis. 1-NP, 1-aminopyrene, and *m*-chloroperoxybenzoic acid were from Aldrich Chemical Co. (Milwaukee, WI). Ethidium bromide, polyethylene glycol 8000, and isopropyl β-D-thiogalactopyranoside (IPTG) were obtained from Sigma (St. Louis, MO). M13 DNA sequencing kit, 5-bromo-4-chloro-3-indolyl β-D-galactopyranoside (X-Gal), 3′→5′ exonuclease-deficient Klenow fragment [KF (exo$^-$)], a modified 3′→5′ exonuclease-free T7 DNA polymerase (Sequenase version 2.0), proteinase K, and *E. coli* single strand binding protein were purchased from US Biochemical Corp. (Cleveland, OH). [α-^{35}S]dATP was from Du Pont New England Nuclear (Boston, MA).

Methods

Unlabeled 1-NOP was synthesized according to published procedure (Howard et al., 1983a). Oligodeoxynucleotides were synthesized on an Applied Biosystems, Inc., Model 380B DNA synthesizer, using the phosphoramidite method. HPLC separations were performed using reverse-phase columns (Phenomenex Ultramex C-18, 4.6 × 250 mm). Bacteriophage M13mp18 DNA was prepared as described (Sambrook et al., 1989).

DNA Modification and Analysis. Fifty micrograms of M13mp18 ss DNA in 50 μL of citric acid/sodium citrate buffer (3 M, pH 5.0) was mixed with varying amounts of [^{3}H]-1-NOP dissolved in 100 μL of DMSO in the presence

of 1 molar equivalent of ascorbic acid. The total volume of the solution was brought to 500 μL with sterile water. Each mixture was purged with nitrogen for ~1 min and then vigorously shaken at 37 °C in the dark for 1.0 h. At 15-, 30-, and 45-min intervals, an additional equivalent of ascorbic acid was added to ensure that most of the 1-NOP was reduced to NHOP. The unreacted chemicals were removed by three consecutive chloroform extractions, and the DNA was precipitated with ethanol. It was redissolved in 10 mM Tris-HCl and 1 mM EDTA, pH 7.4, and dialyzed extensively against the same buffer. Finally, the integrity of the genome was examined by agarose gel electrophoresis. The number of dG^{AP} adducts per DNA molecule was calculated from [^{3}H] content and UV absorption measurements. A portion of adducted DNA was enzymatically hydrolyzed with DNase I, nuclease P1, and acid and alkaline phosphatase and analyzed by reverse-phase HPLC as described by Howard et al. (1983b).

Polymerase Arrest Assay. The appropriate primer (2.5 ng) was annealed to the modified or unmodified DNA (1 μg) by heating at 65 °C for 2 min followed by slow cooling to room temperature over a 30-min period in 10 mM Tris-HCl (pH 7.4), 0.1 mM EDTA, 8 mM $MgCl_2$, 50 mM NaCl, and 10 mM β-mercaptoethanol. In certain experiments, 8 mM $MgCl_2$ was replaced with 0.5 mM $MnCl_2$. Once annealing was complete, DTT to 2 mM and BSA to 100 μg/mL final concentrations were added, followed by 1.5 μM each of dGTP, dATP, and dCTP and 2 μM [α-^{35}S]dATP. Extension of the primer was initiated by KF (exo$^-$) at an ambient temperature in the presence of 0.5 μg of single-strand binding protein to ensure that arrest in DNA synthesis was not due to DNA secondary structures. Primer extension was allowed to continue at 40 °C for an additional 5 min, following which a 15-min chase with 50 μM of each dNTP was carried out. Some polymerase arrest experiments were done with Sequenase version 2.0 rather than KF (exo$^-$). Extension was terminated by adding a "stop" solution containing 95% formamide, 20 mM EDTA, 0.05% Bromophenol blue, and 0.05% Xylene cyanol. The single-strand binding protein was inactivated by adding 0.1 μg of proteinase K, and the mixture was incubated at 65 °C for 20 min. Electrophoresis of an aliquot of these reactions along with a set of dideoxynucleotide sequencing reactions was performed in 8% polyacrylamide gel containing 8 M urea. To quantitate the extent of polymerase arrest, the dry gel was analyzed on a Molecular Dynamics Model 400S PhosphorImager.

SOS Induction and Transformation in E. coli. E. coli cells were grown in 100 mL cultures to 1 × 10^8 cells/mL and then harvested by centrifugation at 5000g for 15 min at 0 °C. The cells were resuspended in equal volume ice-cold deionized water and recentrifuged at 5000g for 30 min. This procedure was repeated except the cells were resuspended in 50 mL of water. The bacterial pellet was resuspended in 1 mL of glycerol/water (10% v/v) and kept on ice until further use. To induce SOS, the following additional steps were introduced after the first centrifugation. The cells were resuspended in 50 mL of 10 mM $MgSO_4$ and treated with an appropriate dosage of UV light (254 nm) in 25 mL aliquots in 150 × 50 mm plastic Petri dishes. Excision repair-deficient cells (DL6) were irradiated in LB rather than $MgSO_4$ because of their high sensitivity to UV light. The cultures were incubated in Luria broth at 37 °C for 40 min (*uvr*$^+$) or 20 min (*uvrA*) in order to express SOS functions maximally. Following SOS induction, these cells were centrifuged, deionized, and resuspended in glycerol/water in a similar manner as described earlier except all manipulations were carried out in subdued light. For each transformation, 40 μL of the cell suspension was mixed with 4 μL (500 ng) of DNA solution and transferred to the bottom of a cold Bio-Rad Gene-Pulser cuvette (0.1 cm electrode gap). Electroporation of cells was carried out in a Bio-Rad Gene-Pulser apparatus at 25 μF and 1.8 kV with the pulse controller set at 200 Ω. Immediately after electroporation, 1 mL of SOC medium was added and the mixture was transferred to a 1.5 mL microcentrifuge tube. Part of the suspension was plated immediately in the presence of the plating bacteria *E. coli* GW5100, IPTG, and X-Gal to determine the number of independent transformants. The remainder of cells was incubated for 1 h at 37 °C to allow for phage replication and subsequently centrifuged at 15000*g* (5 min) to isolate the phage-containing supernatant.

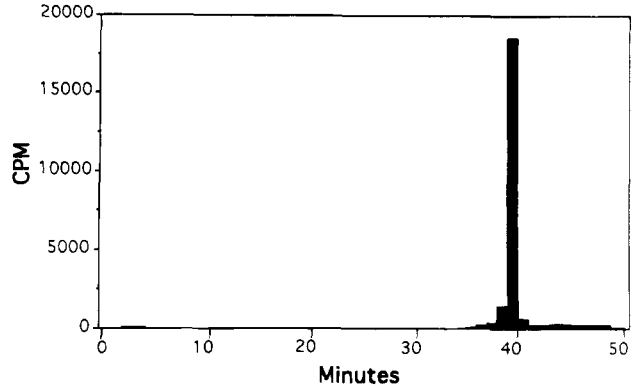

FIGURE 1: HPLC analysis of enzymatically digested NHOP-adducted M13mp18 genome. The DNA was treated with [^{3}H]NHOP and hydrolyzed as described in Materials and Methods. The adducted and unadducted nucleosides were separated on a Phenomenex Ultramex C18 (5 μM) column by eluting with a 30-min linear gradient of 0−20% acetonitrile followed by a 10-min linear gradient of 20−80% acetonitrile in 0.1 M NH_4OAc (pH 6.0) with a flow rate of 1 mL/min; 80% acetonitrile wash was continued for an additional 5 min. No other radiolabeled material eluted with a subsequent wash with 100% acetonitrile. Coinjection of an authentic sample of dG^{AP} indicated that the adduct eluted between 38.5 and 40 min.

Isolation and Identification of Mutants. Each transformation mixture was analyzed by plating progeny phage with GW5100 host cells on indicator plates. Multiple transformations were carried out for each data point. Mutant phage was detected as pale blue or colorless plaques after 18-h incubation at 37 °C followed by 12 h at room temperature. After appropriate dilution, an aliquot of the putative mutant was replated in the presence of the wild type phage in order to eliminate false positives. The mutation frequency (MF) was determined as the number of pale blue and colorless plaques observed divided by the total number of plaques screened. A small batch of ss DNA from each mutant plaque was prepared, and the DNA sequence was determined.

RESULTS

NHOP Modification of ss M13 DNA and Distribution of Adducts. ss M13mp18 was allowed to react under acidic conditions (pH 5.0) with [^{3}H]NHOP generated in situ by ascorbic acid reduction of [^{3}H]-1-NOP. These conditions have been reported to be optimal for generation of the dG^{AP} adducts in DNA (Heflich et al., 1985; Vyas et al., 1993). Part of the adducted ss DNA was digested to the component nucleosides and analyzed by HPLC. More than 95% of the

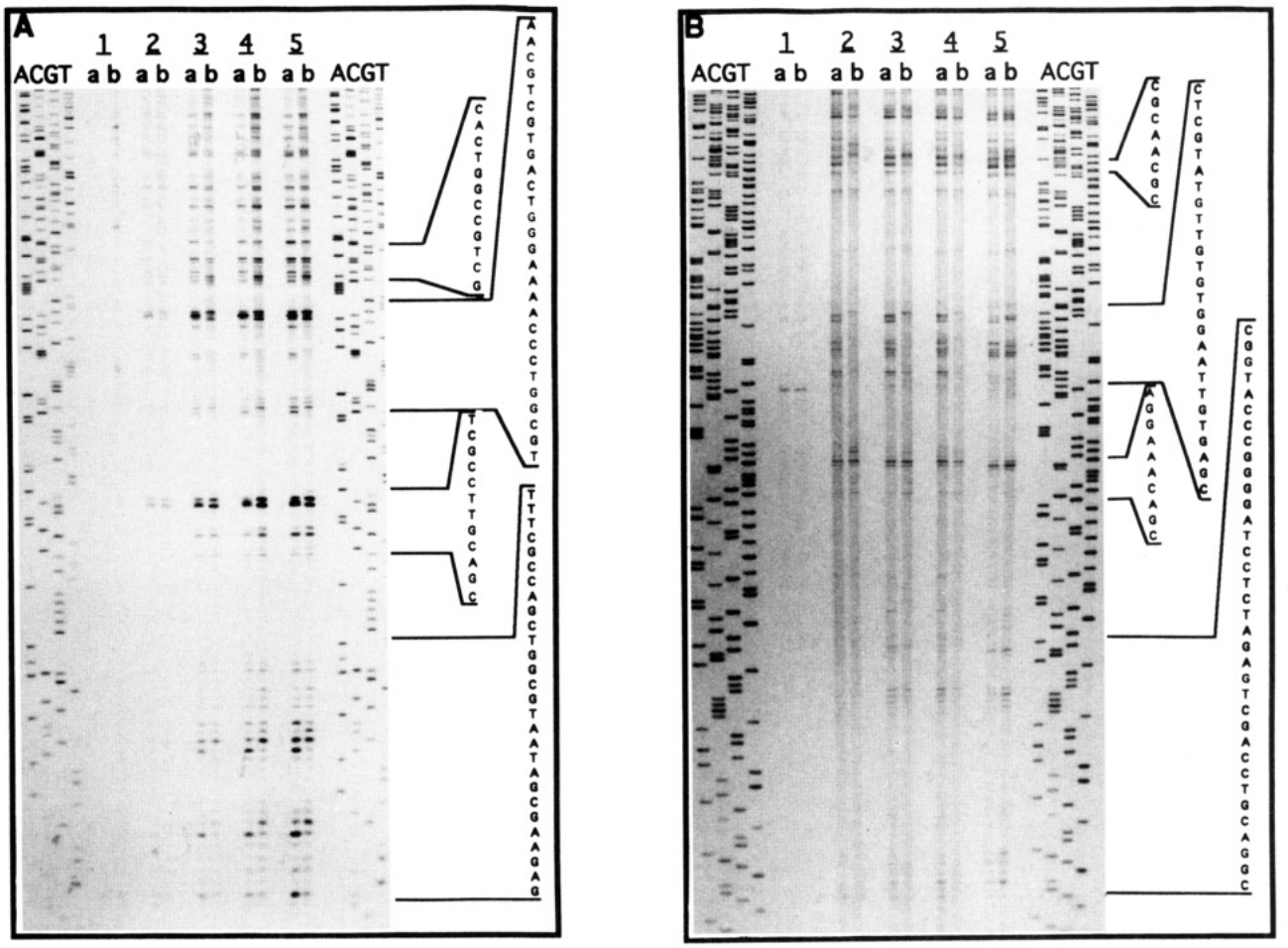

FIGURE 2: Autoradiogram showing in vitro replication analysis of unadducted and adducted ss M13mp18 template in the presence of either Mg^{2+} or Mn^{2+}. In panel A, the primer 5′-CTGTTGG-GAAGGGCG complementary to bases 177−191 was used, whereas in panels B and C, the −40 universal primer 5′-GTTTTCCCAGT-CACGAC complementary to bases 79−95 was employed. Lanes A, C, G, and T represent the standard Sanger sequencing reactions (for example, A implies dideoxyadenosine ladder). Lane 1 in each panel shows the in vitro replication with unadducted M13, whereas lanes 2−5 represent the same with increasing level of dG^{AP} adducts per genome. Panels A and B: lanes 1a−5a display the polymerase blocks with KF (exo$^-$) in the presence of Mg^{2+}, whereas lanes 1b−5b represent the same in the presence of Mn^{2+}. Panel C shows the same except that KF (exo$^-$) was replaced with Sequenase version 2.0. In each case, a section of the relevant DNA sequence of the (+) strand (i.e., complementary sequence to the dideoxy reactions) is shown on the right side of each panel.

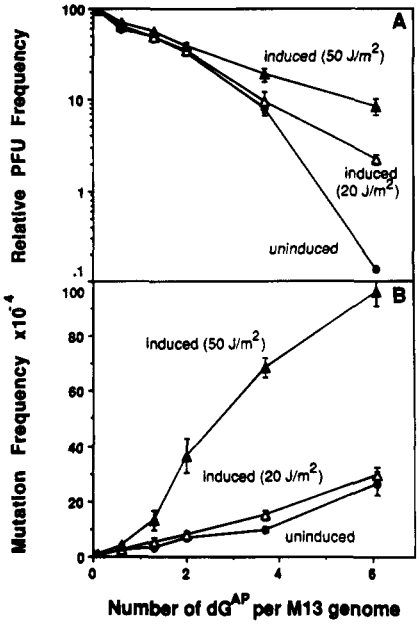

FIGURE 3: Viability and mutation frequency after transfection of adducted ss M13mp18 DNA into SOS-induced (△, 20 J/m^2; ▲, 50 J/m^2) and uninduced (●) DL7 cells. (A) Viability is shown as percentage of total plaques/ng of DNA transfected. (B) MF was determined as the number of colorless or pale blue plaques divided by the total number of plaques screened. Each data point represents the mean ± standard deviation of 3−6 independent experiments. For some points standard deviation was smaller than the symbol.

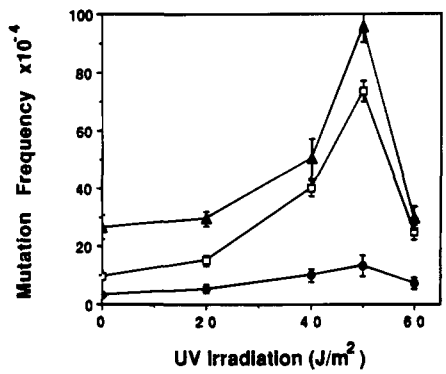

FIGURE 4: Effect of SOS induction on Gua^{AP} mutagenesis in DL7 host cells. Cells were treated with 0, 20, 40, 50, and 60 J/m^2 in $MgSO_4$ (10 mM) and incubated in Luria broth at 37 °C for 40 min in order to express SOS functions maximally. After preparation of these cells as described in Materials and Methods, ss M13mp18 genomes containing an average of 1.3 (●), 3.7 (□), and 6.1 (▲) adducts per genome were used for electroporation. We have also used an additional UV dose of 80 J/m^2; however, viability of the adducted genomes was too low for a reliable estimation of MF. MF was determined as the number of colorless or pale blue plaques divided by the total number of plaques screened. Each data point represents the mean ± standard deviation of 3−6 independent experiments.

^{3}H counts were localized in the dG^{AP} peak as detected by coelution with an unlabeled authentic sample (Figure 1). An unidentified deoxyadenosine adduct is also formed in NHOP reaction with DNA (Kinouchi & Ohnishi, 1986). Although we did not detect any peak either before or after dG^{AP} eluted from the column, a small increase in counts at 44 min was noted, which was <1% of the total ^{3}H counts. Since we did not have a standard of the deoxyadenosine adduct, it is unknown if this small peak could have been due to this adduct. The integrity of the genome was maintained after the modification because no significant nicking was observed by agarose gel electrophoresis either before or after alkali

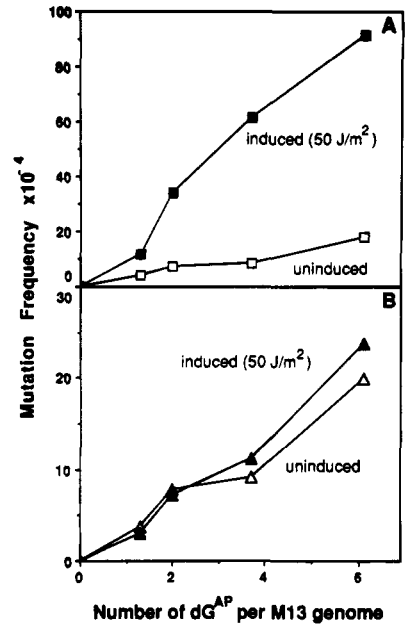

FIGURE 5: Mutation frequency of adducted genome in (A) RW118 with (■) and without (□) UV irradiation (50 J/m^2) and (B) RW120 with (▲) and without (△) UV irradiation (50 J/m^2). Results are the mean of two separate experiments.

treatment (data not shown). To determine the sites of adduction, we have used a polymerase arrest assay that was successfully employed to map several bulky and polymerase blocking lesions (Moore et al., 1981; Ross et al., 1993). In addition, studies in our laboratory suggested that site-specifically incorporated dG^{AP} strongly blocks DNA replication (R. R. Vyas and A. K. Basu, unpublished). As shown in Figure 2, the positions of polymerase arrest bands were nonrandom and they varied in intensity. When polymerase arrest bands were compared with the DNA sequencing ladder, at >95% of the arrest sites there was a Gua either at the arrest site or immediately 5′ to it (i.e., a band was noted in the dideoxy C lane). This is consistent with the notion that DNA synthesis was stopped either opposite dG^{AP} or 3′ to the adduct site. Most of the arrest sites were the same for both KF (exo$^-$) and Sequenase (Figure 2, panels B and C). Irrespective of the extent of treatment, the block sites remained the same. This suggests that the reaction of NHOP with Gua is dependent on the DNA sequence context even in ss DNA. This could be due to local secondary structures, because NHOP reacts preferentially with Gua residues that are in duplex form (Vyas et al., 1993). When the Mg^{2+} ions in the polymerase extension buffer were replaced with Mn^{2+}, some replication blocks were partially or completely alleviated at the site of arrest. However, most arrests reappeared at the base immediately 5′ to the previous arrest site. Only at a very few sites was the arrest completely eliminated. For this experiment, it is important to point out that the heating at 65 °C for 2 min necessary for annealing was unlikely to cause any loss of the adduct, because dG^{AP}-containing DNA fragments are stable after heating at 100 °C for 2 min (S. A. Malia and A. K. Basu, unpublished).

Survival and Mutagenesis of Adducted DNA, and Effects of SOS Functions. The relative plaque forming ability (i.e., the number of infective centers) of the adducted M13 genome was measured following transformation in *E. coli*. As shown in Figure 3A, there was a progressive decrease in plaque forming units (pfu) with increasing modification levels. The number of adducts required to achieve 37% survival, which

constitutes an average of one lethal hit according to the Poisson distribution, was approximately 2 adducts per genome for the excision repair-proficient cell line (DL7). An increased number of pfu from each adducted genome was obtained upon induction of SOS response. Similar results were noted with *uvrA* cells (DL6) (data not shown).

An inverse relationship between plaque forming ability and the MF was observed. As shown in Figure 3B, upon transfection of an M13mp18 genome containing an average of 6.1 adducts per genome in uninduced DL7 cells, MF was 26.4×10^{-4}, whereas for the untreated genome MF was $<0.3 \times 10^{-4}$. When the same host cells were induced for SOS functions with 50 J/m^2 UV light, MF of the adducted genome increased to 95.9×10^{-4}. A 4−7-fold increase in MF was observed for most data points when transformants in SOS-induced DL7 cells were compared with that of uninduced cells (Figure 3B). The results in *uvrA* cells (DL6) were similar, although the extent of increase in both survival and mutagenesis, upon induction of SOS response, was less pronounced (data not shown).

The relationship between the UV dosage and MF was established for DL7 cells at three different levels of adduction. The UV irradiation dose of 50 J/m^2 was optimal for all three adducted genomes (Figure 4), and at a higher dosage, the MF decreased instead of reaching a plateau. Similar MF versus UV curve was noted with the C8-Gua adduct of AF, except that the optimal UV dosage was 30−35 J/m^2 (Bichara & Fuchs, 1985; Gupta et al., 1988).

The requirement of SOS functions for the mutagenesis was also shown using two isogenic strains, RW118 and RW120. The *umuDC* operon was deleted in RW120 in which the SOS functions cannot be induced. As shown in Figure 5A, up to a 5-fold increase in MF was observed upon UV irradiation (50 J/m^2) when adducted genomes were transfected in RW118. By contrast, there was no difference in mutagenesis in RW120 by UV irradiation (Figure 5B).

Spectrum of Reductively Activated 1-NP-Induced Mutations. The DNA sequence analysis of the mutants collected during mutation frequency analysis from several sets of transformations was carried out. An area between bases −86 and +179 that codes for the regulatory region and a part of the N-terminal segment of β-galactosidase was analyzed using two different primers. A total of 390 individual mutants was used for sequence analysis, and mutations were noted in 171 (44%) of these mutants. This percentage is in accord with the fact that we have sequenced only part of the β-galactosidase insert. Other workers also noted that mutations in *lacZ* beyond the region sequenced can affect β-galactosidase activity and probably account for the mutants in which sequencing revealed no change in DNA sequence (e.g., Gupta et al., 1988; Lasko et al., 1988). Only 5 spontaneous mutants of the solvent control was determined because of the low frequency of spontaneous mutations. For example, without SOS, the MF of adducted DNA containing 6.1 adducts per genome was >50 times that of control unadducted DNA. With SOS, the MF of the same DNA was as high as 200-fold that of control. Since the MF of the progeny phage from the adducted DNA were 1−2 orders of magnitude higher than the same from control DNA, it is reasonable to assume that the mutants were mainly derived from lesions induced by reductively activated 1-NP. The major types of mutations in both SOS-induced and uninduced cells were point mutations although large deletions ranging

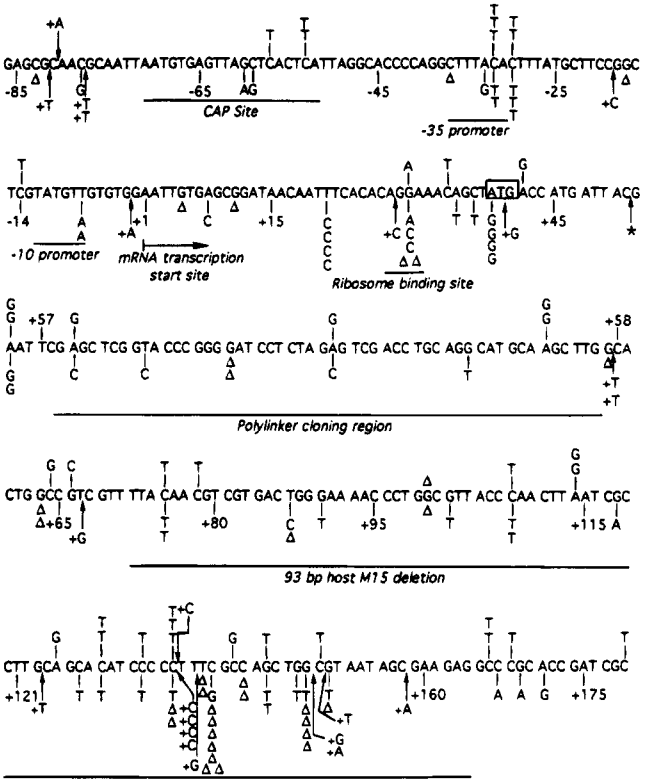

FIGURE 6: Mutational spectra generated by reductively activated 1-nitropyrene. The mutations above the M13 sequence represent the mutations in uninduced cells whereas the mutations below were obtained from SOS-induced cells. The base numbering begins at the start of transcription so that A of the initiation codon (shown inside a rectangle) is base 39. Also, the polylinker site was ignored in this numbering system so that the data from this article can be easily compared with mutation data in any M13mp vector. The asterisk between positions 52 and 53 indicates a CG-to-GAC base change. The symbol Δ implies a one-base deletion. When a −1 or +1 frame shift occurred in a run of two or more of the same base, the exact location of the base deleted or added is unknown.

from 19 to >300 nucleotides have been detected in both SOS-induced (11%) and uninduced (16%) cells.

Without SOS, the major proportion of mutants were C→T (24/50) and A→G (10/50) transitions (Table 1). C→T mutations were unexpected because Cyt adducts have never been reported to form with reductively activated 1-NP. We showed, however, that the C→T transitions occurred due to Cyt deamination during nitroreduction and that these events were unrelated to dG^{AP} mutagenesis (Malia & Basu, 1994). Briefly, genetic evidence of deamination of Cyt was obtained by transfecting the DNA into two isogenic strains, in which one carried a defect in the *ung* gene product, uracil DNA glycosylase, and therefore was inefficient in excising uracil residues from DNA. Both survival and mutagenesis of each adducted genome increased in the *ung*$^-$ strain when compared with the same in the *ung*$^+$ strain. Also, the difference in MF increased with increasing chemical treatment. At the highest level of adduction, when the genome contained an average of 6.1 Gua^{AP}, there was a 20-fold enhancement in MF in the *ung*$^-$ strain relative to the repair-proficient one. However, the survival and mutagenesis of the M13 DNA were similar when mannitol was present during DNA adduction. Since mannitol is a well-known radical scavenger, this suggests involvement of a radical species in Cyt deamination. A direct evidence of Cyt deamination was obtained by exposing 2′-deoxycytidine to the conditions of reduction of 1-NOP by ascorbic acid. HPLC analysis

Table 1: Summary of All Mutations Induced by Reductively Activated 1-NP[a]

types of mutation		−SOS	+SOS
base substitutions:			
A	→C	0	3
	→G	10	8
	→T	0	1
C	→A	0	1
	→G	2	3
	→T	24	14
G	→A	1	5
	→C	1	2
	→T	1	8
T	→A	0	2
	→C	0	6
	→G	0	0
one-base deletions:			
A		0	0
C		0	13
G		1	17
T		0	3
one-base insertions:			
A		1	3
C		1	6
G		0	4
T		0	8
other[b]		0	1
large deletions: (19−330 bases)		8	13

[a] A compilation of data from Figure 6. Three additional mutations in SOS-induced cells, a G→A, a G deletion (both at position −121), and a T insertion between a G and C (at positions −120 and −119, respectively), have been included. [b] The CG-to-GAC mutation has been included in this category.

showed that the ratio 2′-deoxyuridine/2′-deoxycytidine increased continuously with time over a 6-h period. 2′-Deoxyuridine was undetectable, however, when either 1-NOP or ascorbic acid was excluded from the reaction mixture. Although Ade deamination was not investigated, we suspect that the A→G transitions also occurred as a result of deamination of Ade to inosine. Alternatively, it could have been the consequence of an unidentified Ade adduct.

When SOS functions of the host cells were induced, one-base deletions and one-base insertions were detected at a much higher frequency. Together, +1 and −1 frame shifts contributed to 54/107 of point mutations in SOS-induced cells compared to 3/42 in uninduced cells. In addition, upon induction of SOS, twice as many G→A transitions and 3 times as many G→T transversions were detected. Figure 6 displays the mutational spectra both in the presence and in the absence of SOS functions of the host cells. Of the five spontaneous mutants, which were not included in this figure, two exhibited A→T transversions (at position −171 and at the fourth A in the polylinker region) and one had a C→A transversion (at position +111). Large deletions were detected in the remaining two mutants of the solvent control.

An analysis of the local sequences surrounding the mutated bases suggested that only a fraction of the mutants were targeted at Gua residues, although >95% adduction occurred at Gua sites. However, we already pointed out that the C→T and A→G events were unlikely to be the consequence of Gua adduction. If C→T and A→G transitions are excluded from the analysis, most mutations were either at Gua residues or at their immediate neighbor. Specifically, 18% and 19% of the point mutations other than C→T and A→G transitions were at the 5′ and 3′ base to a Gua, respectively, whereas 51% were targeted at Gua.[2] Most insertions were next to a Gua, as expected. However, 13 of 34 one-base deletion events involved a loss of Cyt, of which 11 Cyt residues were located next to a Gua. Since no Cyt damage other than the deamination product, uracil, has ever been detected by reductively activated 1-NP, it is unlikely that these Cyt deletions are targeted mutations. This suggests that Gua^{AP} can probably induce untargeted mutagenesis, which involves either a 5′ or 3′ neighbor of the adducted Gua. In ds DNA, such a Cyt deletion can be easily misinterpreted as a Gua deletion. Because of an inherent ambiguity in untargeted mutagenesis, we did not attempt to analyze the sequence environment rigorously; for example, a comparison of the MF in different NGN triplets was not carried out. Nevertheless, certain sequence context effects are noteworthy. It is interesting that most one-base deletions were at 5′-GC, 5′-CG, or 5′-GG sites. In addition, all of the +1 insertion of Thy residues and most of the other +1 insertions occurred at 5′-CG or 5′-GC sequences. For the G→A and G→T base substitutions as well, a neighboring Cyt or Gua appears to be common.

Relationship between Polymerase Arrest Sites and Mutational Sites. The results shown thus far suggest strongly that dG^{AP} was the major adduct formed in the M13 DNA, and the enhancement of mutagenesis in SOS-induced cells is likely to be the consequence of this DNA adduct. The polymerase arrest assay suggested the sites where this adduct was located at a high frequency. We attempted to find out whether there is a reasonable association between the sites at which point mutations were observed with the sites where polymerase arrests occurred. In Figure 7 the polymerase arrest sites are shown as histograms above the DNA strand whereas the point mutations, irrespective of whether they were derived from SOS-induced or uninduced cells, are displayed below the DNA strand. The C→T transitions have not been included in this diagram because most of these events relate to Cyt deamination which should not be inhibitory to DNA replication. As shown in Figure 7, mutations were detectable in most arrest sites, but none of the mutations were associated with one of the two major arrest sites at bases 78−80. Another major arrest site between bases 117 and 119, which yielded only one mutagenic event, was not a hotspot either. Nevertheless, polymerase arrest bands were found for 77 of 105 point mutations. Most of these mutations were specifically at the arrest site or immediately 3′ to it. Although only ~25% of the 303 bases corresponded to block sites, 73% of mutations occurred at sites where polymerase arrests occurred. However, like the C→T transitions, the association between A→G transition and polymerase block sites was poor. It is conceivable that the Ade damage (such as the deamination product, inosine) is not a major polymerase blocking lesion. If A→G mutations are excluded from the analysis, nearly 80% of the mutational sites corresponded to polymerase block sites. This indicates a reasonable, albeit not excellent, association between a mutational site and the presence of an adduct. However, there was no pattern that would enable

[2] For this calculation, all one-base insertions next to a Gua, being either 5′ or 3′ to it, have been considered as "targeted" mutations. Likewise, the one-base insertions between one and two bases 3′ to a Gua have been counted as mutations at the 3′ base. When a mutation other than C→T transition was detected at a nucleotide between two Gua (i.e., N in a 5′-GNG sequence), it was arbitrarily counted as 3′ to a Gua.

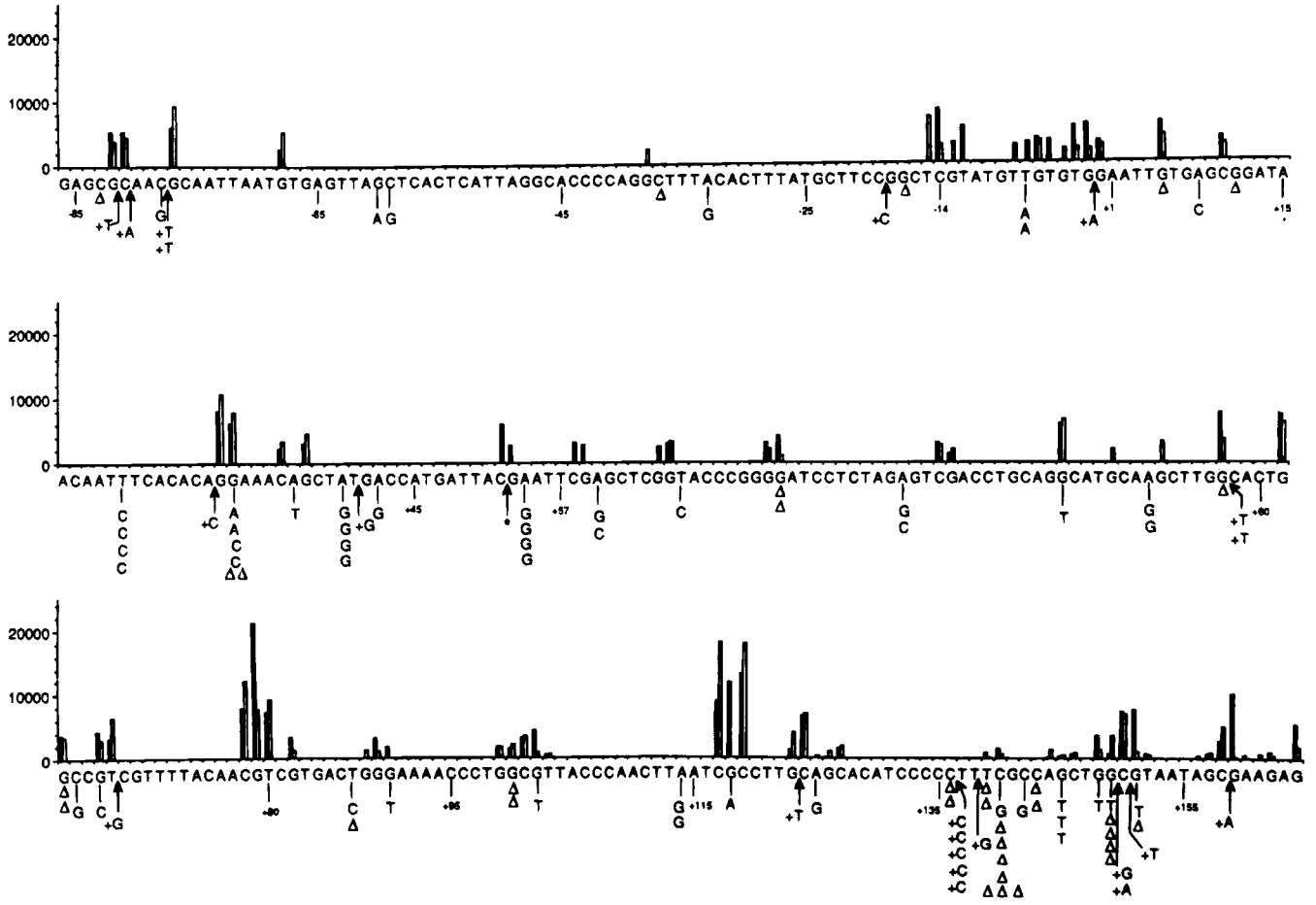

FIGURE 7: The M13mp18 sequence between bases −86 and 164 displays the sites of polymerase arrests with KF (exo$^-$) as histograms above the DNA sequence, whereas the sites where point mutations (excluding C→T) were detected are shown below it. Polymerase arrest experiments performed in the presence of Mg^{2+} and Mn^{2+} as shown in panels A and B of Figure 2 (lanes 5a and 5b) are displayed as solid bars and open bars, respectively. The nucleotide location corresponds to the position above the first digit of each number. The asterisk between positions 52 and 53 indicates a CG-to-GAC base change. The symbol Δ implies a one-base deletion.

us to predict a mutational hotspot from a polymerase arrest assay.

DISCUSSION

A direct reaction of the reductively activated 1-NP with DNA generated Gua^{AP} as the predominant DNA-bound 1-aminopyrene derivative. Gua^{AP} was shown to be a strong block of replication, and complete inactivation of an M13 genome can be induced with 2 such adducts per genome. If this inactivation kinetics is compared with C8-Gua-AF that requires 6 adducts per genome for complete inactivation, Gua^{AP} appears to cause significantly more lethal damage than the AF adduct (Gupta et al., 1988).

Like many other chemical mutagens, mutagenic specificity of Gua^{AP} is unique. It can induce a variety of mutations that include large deletions, one-base additions and deletions, and G→A and G→T base substitutions. Most mutations were clustered in a few sites. When these mutations were compared with previous studies in bacterial and mammalian cells, there appears to be a major difference in how 1-NOP is activated and how the adducts are processed by enzymes in mammalian cells and in bacteria. Frame shift mutations and especially one-base additions and deletions are the major events in bacteria. As far as frame shift mutagenesis is concerned, it is interesting that Stanton et al. (1988) found mostly one-base additions whereas Melchoir et al. (1994) exclusively detected one-base deletions. We have observed both events at significant frequency. These differences probably reflect many differences between these experimental systems. Base pair substitutions, on the other hand, are the principal class of mutations in mammalian cells. Many mutations in the present study were base substitutions, but specifically C→T transitions occurred most frequently. The C→T substitutions, despite their lack of relationship with Gua^{AP}, are an integral part of the mutation spectrum induced by reductively activated 1-NP. Other base substitutions detected in the present study include G→T transversions and G→A transitions. Several T→C, A→G, and C→G were also observed. For the G→T transversions, we cannot rule out that a fraction of these could have arisen via deamination of Gua to xanthine followed by depurination. It is noteworthy that one-base addition and deletion events were induced almost exclusively when SOS was induced. Mutations at Thy residues were noted also upon induction of SOS. In addition, both G→A transitions and G→T transversions increased approximately 2−3-fold. Most other mutations remained the same in SOS-induced cells. Therefore, reductively activated 1-NP mutagenesis can be separated into SOS-independent and SOS-dependent components. Assuming that Gua^{AP} was responsible for most of the SOS-dependent mutations, it would appear from our data that this adduct can cause both targeted and untargeted mutagenesis.

The DNA polymerase arrests at the site of bulky carcinogen−DNA adducts have been used by others to investigate

the sequence specificity of binding by reactive carcinogen metabolites (Moore et al., 1981; Ross et al., 1993). Some of these adducts, if unrepaired, can give rise to mutations. In the present study, we have compared the sites of adduct formation as suggested by the polymerase arrest assay with the mutational sites. Interpretation of these results is complicated because many mutations are not phenotypically detectable and both DNA repair and mutagenesis are dependent on the sequence context. The major polymerase arrest sites in this study were not mutational hotspots, which is consistent with the suggestion that certain sequences are mutation prone (Benzer, 1961). Even so, nearly 80% of the point mutations (except for C→T and A→G transitions) were at polymerase arrest sites. It is intriguing that the sequence TCGCC between bases 139 and 143 displayed a low adduction level and a one-base deletion hotspot whereas the same pentanucleotide sequence at bases 115−119 was a major arrest site with only one detectable mutation. This pentanucleotide sequence is also present at position 176−180 where no deletion was detected. It is also noteworthy that mutations were detected at both 5′ and 3′ bases but not at the Gua at position 141. Only in this site, however, one can postulate a hairpin loop between bases 138 and 154 (i.e., 5′-TTCGCCAGCTGGCGTAA sequence can fold as a hairpin structure if the third T from the 3′ end loops out). A large fraction of point mutations was detected in this region. Frame shift mutagenesis by C8-Gua-AAF at a palindromic sequence such as GGCGCC by an insertion−denaturation model has been proposed (Fuchs & Daune, 1972). An analogous mechanism may also be postulated for Gua^{AP} mutagenesis at this site.

In summary, our results suggest that Gua^{AP} is a polymerase blocking lesion. In addition, it is mutagenic, especially when SOS functions of the host cells are induced. The mutagenic specificity of Gua^{AP} is unique: most frequent mutations are one-base additions and deletions, large deletions, and G→A and G→T base substitutions. An interesting point noted in this study is that Gua^{AP}, unlike many well-studied carcinogen−DNA adducts, induced mutations both at the adduct site and at the base located next to it. To address these and other intriguing aspects of dG^{AP} mutagenesis, site-specific mutagenesis experiments are in progress in our laboratory.

ACKNOWLEDGMENT

We are grateful to Dr. F. A. Beland (NCTR) for the gift of [^{3}H]-1-NOP and to Dr. J. M. Essigmann (MIT) for allowing us to use the PhosphorImager. We thank R. R. Vyas and S. Lizarraga (UConn) for expert technical assistance.

REFERENCES

Bell, D. A., Levin, J. G., & DeMarini, D. M. (1991) *Mutat. Res. 252*, 35−44.

Benzer, S. (1961) *Proc. Natl. Acad. Sci. U.S.A. 47*, 403−415.

Bichara, M., & Fuchs, R. P. P. (1985) *J. Mol. Biol. 183*, 341−351.

Djurić, Z., Fifer, E. K., Howard, P. C., & Beland, F. A. (1986) *Carcinogenesis 7*, 1073−1079.

El-Bayoumy, K. (1992) *Chem. Res. Toxicol. 5*, 585−590.

El-Bayoumy, K., & Hecht, S. S. (1984) *Cancer Res. 44*, 4317−4322.

El-Bayoumy, K., Rivenson, A., Johnson, B., DiBello, J., Little, P., & Hecht, S. S. (1988) *Cancer Res. 48*, 4256−4260.

Fuchs, R. P. P., & Daune, M. (1972) *Biochemistry 11*, 2659−2666.

Gupta, P. K., Lee, M.-S., & King, C. M. (1988) *Carcinogenesis 9*, 1337−1345.

Heflich, R. H., Howard, P. C., & Beland, F. A. (1985) *Mutat. Res. 149*, 25−32.

Heflich, R. H., Fullerton, N. F., & Beland, F. A. (1986) *Mutat. Res. 161*, 99−108.

Hirose, M., Lee, M.-S., Wang, C. Y., & King, C. M. (1984) *Cancer Res. 44*, 1158−1162.

Howard, P. C., & Beland, F. A. (1982) *Biochem. Biophys. Res. Commun. 104*, 727−732.

Howard, P. C., Beland, F. A., & Cerniglia, C. E. (1983a) *Carcinogenesis 4*, 985−990.

Howard, P. C., Heflich, R. H., Evans, F. E., & Beland, F. A. (1983b) *Cancer Res. 43*, 2052−2058.

Howard, P. C., Flammang, T. J., & Beland, F. A. (1985) *Carcinogenesis 6*, 243−249.

King, C. M. (1988) *Health Effect Institute Research Report No. 16*, pp 1−31, Health Effects Institute, Cambridge, MA.

Kinouchi, T., & Ohnishi, Y. (1986) *Microbiol. Immunol. 30*, 979−992.

Lasko, D. D., Harvey, S. C., Malaikal, S. B., Kadlubar, F. F., & Essigmann, J. M. (1988) *J. Biol. Chem. 263*, 15429−15435.

Malia, S. A., & Basu, A. K. (1994) *Chem. Res. Toxicol. 7*, 823−828.

McGregor, W. G., Mahar, V. M., & McCormick, J. J. (1994) *Cancer Res. 54*, 4207−4213.

Melchior, W. B., Jr., Marques, M. M., & Beland, F. A. (1994) *Carcinogenesis 15*, 889−899.

Moore, P. D., Bose, K. K., Rabkin, S. D., & Strauss, B. S. (1981) *Proc. Natl. Acad. Sci. U.S.A. 78*, 110−114.

Newton, R. K., Mittelstaedt, R. A., Manjanatha, M. G., & Heflich, R. H. (1992) *Carcinogenesis, 13*, 819−825.

Ohnishi, Y., Kinouchi, T., Manabe, Y., Tsutsui, H., Otsuka, H., Tokiwa, H., & Otofuji, T. (1985) in *Short Term Genetics Bioassays in the Evaluation of Complex Environmental Mixtures* (Waters, M. D., Shandhu, S. S., Lewtas, J., Claxton, L., Strauss, G., & Nesnow, S., Eds.) pp 195−204, Plenum Press, New York.

Pitts, J. N., Jr., van Cauwenberghe, K. A., Grosjean , D., Schmid, J. P., Fitz, D. R., Belser, W. L., Jr., Knudson, G. B., & Hynds, P. M. (1978) *Science 202*, 515−519.

Rosenkranz, H. S. (1982) *Mutat. Res. 101*, 1−10.

Rosenkranz, H. S., & Mermelstein, R. (1983) *Mutat. Res. 114*, 217−267.

Rosenkranz, H. S., McCoy, E. C., Sanders, D. R., Butler, M., Kiriazides, D. K., & Mermelstein, R. (1980) *Science 209*, 1039−1043.

Ross, H., Bigger, C. A. H., Yagi, H., Jerina, D. M., & Dipple, A. (1993) *Cancer Res. 53*, 1273−1277.

Sambrook, J., Fritsch, E. F., & Maniatis, T. (1989) in *Molecular Cloning: A Laboratory Manual*, Cold Spring Harbor Laboratory Press, Cold Spring Harbor, NY.

Schuetzle, D. (1983) *Environ. Health Perspect. 47*, 65−80.

Stanton, C. A., Chow, F. L., Phillips, D. H., Grover, P. L., Garner, R. C., & Martin, C. N. (1985) *Carcinogenesis 6*, 535−538.

Stanton, C. A., Garner, R. C., & Martin, C. N. (1988) *Carcinogenesis 9*, 1153−1157.

Vyas, R. R., Nolan, S. J., & Basu, A. K. (1993) *Tetrahedron Lett. 34*, 2247−2250.

Wang, C. Y., Lee, M.-S., King, C. M., & Warner, P. O. (1980) *Chemosphere 9*, 83−87.

Yang, J.-L., Maher, V. M., & McCormick, J. J. (1988) *Mol. Cell. Biol. 8*, 3364−3372.

BI942015D